

+ $D_{\alpha\beta}^C(\vec{q}; l_3, l_3'; j, j')$ with $\vec{q}=0$.

¹⁴This classification of the normal modes into four types is strictly valid only at $Q=0$, but it remains approximately valid for Q as large as 0.1. For larger values of Q , many modes interact and exchange characters, so the classification is generally no longer useful.

¹⁵The lowermost TO bulk mode gradually assumes the character of a surface mode as the slab thickness in-

creases. This mode will be discussed in more detail below.

¹⁶The optical properties are determined from the $\vec{q}=0$ unretarded normal modes (cf. Ref. 13).

¹⁷M. Haas, Phys. Rev. **117**, 1497 (1960).

¹⁸G. O. Jones, D. H. Martin, P. A. Mawer, and C. H. Perry, Proc. Roy. Soc. (London) **A261**, 10 (1961).

Pyroelectric Coefficient of Lithium Sulfate Monohydrate (4.2-320 °K)

Sidney B. Lang

Department of Chemical Engineering, McGill University, Montreal 101, Quebec, Canada

(Received 12 October 1970)

The pyroelectric coefficient (at constant stress) of lithium sulfate monohydrate was measured over the temperature range 4.2–320°K, in order to resolve a discrepancy between the results of Ackermann and those of Gladkii and Zheludev, and to extend the data to below 88°K. The pyroelectric coefficient was observed to change sign at 106°K in agreement with the results of Gladkii and Zheludev. The coefficient passed through a broad extremum at 50°K and approached zero at 4.2°K. The primary and secondary pyroelectric coefficients were calculated over the temperature range; their cancellation at 106°K causes the sign change in the pyroelectric coefficient at constant stress. The secondary coefficient is positive at all temperatures, but the primary coefficient changes sign at 158°K. The Born lattice-dynamical theory of the primary pyroelectric effect was extended to include contributions due both to the acoustical and to the optical spectra of a material. A Debye temperature and five Einstein temperatures calculated from heat-capacity data were used to derive an analytical expression for the primary pyroelectric coefficient.

INTRODUCTION

The first measurements of the pyroelectric coefficient of lithium sulfate monohydrate (LSM) were published by Ackermann in 1915.¹ He determined the pyroelectric coefficient (at constant stress) at discrete temperature values between 23 and 352°K, using a static technique. He found that the coefficient increased monotonically with increasing temperature, with no change in sign at any temperature. Recently Gladkii and Zheludev² repeated the measurements down to 88°K, observing an anomalous change in sign at about 110°K. To resolve the discrepancy, we repeated the measurements, extending the temperature range down to 4.2°K in order to observe the very-low-temperature behavior of the pyroelectric coefficient. The measurements reported here are the first continuous ones over a broad temperature range ever determined on a pyroelectric but nonferroelectric material. Using published piezoelectric, elastic, thermal-expansion, and heat-capacity data, the pyroelectric coefficients were resolved into the primary and secondary components. An expression for the primary pyroelectric coefficient was derived by means of an extension of the Born lattice-dynamics theory of pyroelectricity.

LSM is a monoclinic crystal, point group 2, with

the lattice parameters³ $a=8.18 \text{ \AA}$, $b=4.87 \text{ \AA}$, $c=5.45 \text{ \AA}$, and $\beta=107.3^\circ$. Bechmann⁴ has published piezoelectric and elastic compliance constants referred to a set of axes in which z is collinear with a , x lies in the obtuse angle between a and c , and y is parallel to b , but is directed so as to make a left-handed set of coordinates with x and z . Although this usage is not strictly according to the IRE convention,⁵ Bechmann's system has been adopted in the literature⁶ and it will be used here. Calculations described later in this report utilized the elastic compliance coefficients (s), the piezoelectric stress coefficients (d), their temperature dependencies, and the thermal-expansion coefficients (α). These coefficients, corresponding to the coordinate system described above, were calculated from the original references.^{3,7} There were a few minor discrepancies between some calculated values and those reported in Landolt-Börnstein,⁴ the differences probably being the result of round-off errors.

EXPERIMENTAL METHOD AND RESULTS

The pyroelectric coefficient was determined at constant stress using the dynamic technique of Lang and Steckel.⁸ In this method, the coefficient is calculated from the pyroelectric voltage produced as the temperature of the material under study is

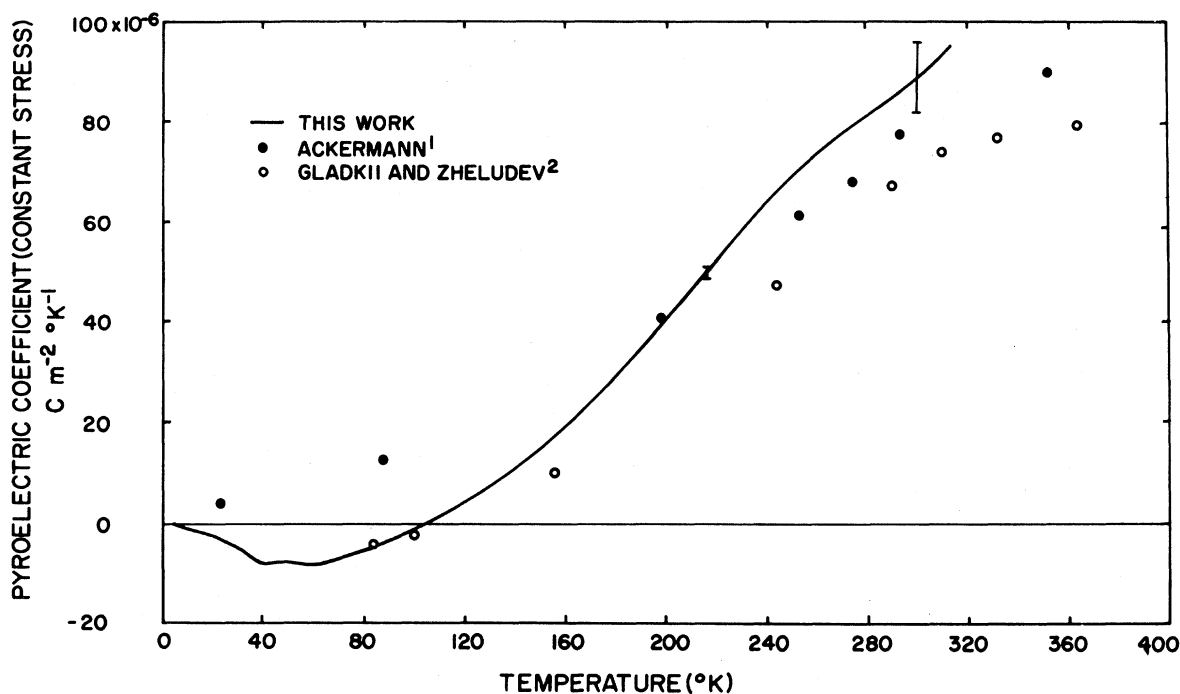


FIG. 1. Pyroelectric coefficient (at constant stress) of lithium sulfate monohydrate. The error bars indicate ± 1 standard deviation. The larger errors near 300 °K were caused by difficulties in controlling the rate of temperature change.

increased or decreased continuously. This method yields continuous rather than discrete data. The sample was held between spring-loaded gold-plated electrodes in an evacuated tube. The tube could be immersed in either a liquid-nitrogen or a liquid-helium storage Dewar. The temperature was observed with either a platinum or a germanium resistance thermometer, depending upon the temperature range. The pyroelectric voltage was measured with a vibrating-reed electrometer shunted with a calibrated $10^{10}\text{-}\Omega$ resistor. Details of the experimental apparatus and techniques are described elsewhere.^{9,10}

The pyroelectric sample used was a 0.64-cm-o.d. by 0.32-cm-thick disk cut from a single crystal of LSM. The flat surfaces of the disk were parallel to the (010) crystallographic planes. The orientation of the sample was verified both by observing extinction with a polarizing microscope and by examining backreflection Laue x-ray photographs. The flat surfaces of the disk were coated with silver paint to ensure good electrical contact.

The results of our measurements and those of Ackermann and Gladkii and Zheludev are shown in Fig. 1. We observed a change in sign of the pyroelectric coefficient at 106 °K, in excellent agreement with the results of Gladkii and Zheludev. Below the sign change, the coefficient passed through a broad extremum at about 50 °K and

reached a minimum value of about $-0.1 \mu\text{C m}^{-2} \text{ }^\circ\text{K}^{-1}$ at 4.2 °K.

INTERPRETATION OF SIGN REVERSAL

The reversal of the sign of the pyroelectric coefficient is a relatively rare phenomenon. This effect has been observed in only three other materials: 5-chlorosalicylideneaniline,¹¹ barium titanate ceramic,¹⁰ and barium nitrate.² We will consider three possible explanations for the sign reversal.

(a) *Metastable phase transformation.* A sign reversal attributed to a metastable phase transformation was observed when the temperature of 5-chlorosalicylideneaniline was varied rapidly. However, the pyroelectric effect in LSM was not a function of rate or sign of temperature change, as was the effect in 5-chlorosalicylideneaniline. Therefore, we exclude this possibility.

(b) *Phase transformation.* The spontaneous polarization of a pyroelectric material may increase or decrease abruptly over a very narrow temperature span if the material undergoes a phase transformation at that point. The pyroelectric coefficient is related to the spontaneous polarization by the following equation:

$$p = \left(\frac{\partial P_s}{\partial T} \right)_{E, \sigma}, \quad (1)$$

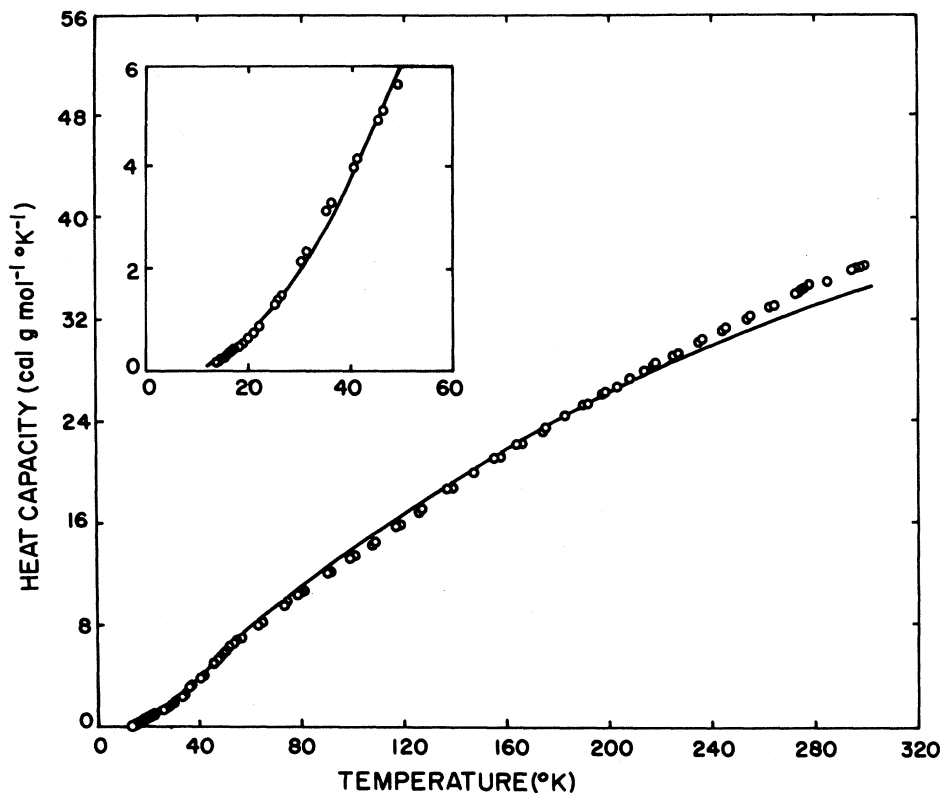


FIG. 2. Heat capacity (at constant pressure) of lithium sulfate monohydrate. The theoretical curve consists of the sum of one Debye function and five Einstein functions, and includes a factor to correct from constant-volume heat capacity to constant pressure. The characteristic temperatures were selected so as to minimize the sum of squares of the relative differences between the experimental points and the theoretical curve rather than the sum of squares of the absolute differences. This improved the data fit at low temperatures as shown in the inset. The average standard deviation per point was 4.5%.

where p , P_s , T , E , and σ represent the pyroelectric coefficient, spontaneous polarization, temperature, electric field, and elastic stress, respectively. The spontaneous polarizations of all three ferroelectric phases of barium titanate ceramic decreased with increasing temperature.¹⁰ However, the spontaneous polarization increased at the *rhombohedral-orthorhombic transition*, resulting in two successive pyroelectric coefficient sign reversals. No low-temperature x-ray-diffraction data are available on LSM, so the possibility of phase transformations cannot be excluded. However, the heat capacity of LSM,¹² shown in Fig. 2, appears to be a very well-behaved function of temperature, with no anomalies. Thus a phase transformation is unlikely.

(c) *Cancellation of primary and secondary pyroelectric coefficients.* The remaining interpretation is based on the fact that the measured pyroelectric coefficient (at constant stress) is the sum of the coefficient at constant strain (primary effect) and the piezoelectric effect due to thermal strain (secondary effect). This relationship can be expressed

by the tensor equation¹³

$$\begin{array}{ccccc}
 p_i^\sigma & = & p_i^\epsilon & + & d_{ijk}^T C_{jklm}^T \alpha_{lm}^\sigma \\
 \text{(total} & & \text{(primary} & & \text{(secondary effect)} \\
 \text{effect)} & & \text{effect)} & & \\
 & & & & \text{(at constant electric field),} \quad (2)
 \end{array}$$

where p_i^σ and p_i^ϵ denote the pyroelectric coefficients measured at constant stress and strain, respectively; d_{ijk}^T represents the piezoelectric tensor (electric displacement/unit stress) at constant temperature; C_{jklm}^T represents the elastic stiffness tensor at constant T ; and α_{lm}^σ represents the thermal expansion tensor at constant σ . All terms in Eq. (2) are at constant electric field. If, at a particular temperature the two terms on the right-hand side of Eq. (2) become equal in absolute magnitude but opposite in sign, the pyroelectric coefficient at constant stress will be zero. The primary and secondary pyroelectric coefficients of barium titanate,¹⁴ several lead-zirconate-titanate

ceramics,¹⁵ and even animal bone¹⁶ have opposite signs but unequal absolute magnitudes at room temperature.

It is possible to resolve the pyroelectric coefficient of LSM at constant stress into the primary and secondary effects over a broad range of temperature if the temperature dependencies of the elastic, piezoelectric, and thermal expansion coefficients are known. Unfortunately, the only experimental measurements available on these properties were made in the range 293–323 °K.

The following procedures were used to estimate the temperature dependencies of the parameters in Eq. (2).

(i) The elastic compliance and piezoelectric constants were assumed to vary linearly with temperature at the rates measured in the temperature range 293–323 °K. The data used were based on the values of Bechmann⁴ as described above. The elastic stiffness matrix at any temperature was computed by inverting the elastic compliance matrix.

(ii) The temperature dependency of the volumetric thermal-expansion coefficient was calculated by the use of the Grüneisen relation and the thermodynamic relation between heat capacities at constant pressure (C_p) and at constant volume (C_v),¹⁷

$$\alpha_v = \gamma C_v / BV, \quad C_p - C_v = \alpha_v^2 BVT, \quad (3)$$

where α_v , γ , B , and V are the volumetric thermal-expansion coefficient, Grüneisen parameter, bulk modulus, and molar volume, respectively.

A Grüneisen parameter of 0.522 at 298 °K was found using thermal-expansion data⁷ and constant-pressure heat-capacity measurements.¹² The Grüneisen parameter of LSM is lower than those of alkali halides¹⁷ because of the relatively low thermal expansion and high heat capacity of LSM. The use of a single Grüneisen parameter for a highly anisotropic material is probably an oversimplification. However the calculated parameter is only used for estimating the temperature dependence of the thermal-expansion coefficients. It is not considered to have any other physical significance. The Grüneisen parameter of LSM was assumed to be independent of temperature. The volumetric thermal-expansion coefficient of LSM was then calculated as a function of temperature from Eq. (3). By also assuming that each of the relative temperature derivatives of the three *principal* expansion coefficients was equal to the relative derivative of the volumetric coefficient and that the orientations of the *principal* axes were temperature independent, the linear expansion coefficients could be estimated as functions of temperature.

Equation (2) was expanded and the tensor notation was replaced with the conventional matrix nota-

tion.¹³ Calculations were made of the secondary pyroelectric coefficient at a number of discrete points as shown in Fig. 3. Note that the secondary pyroelectric coefficient must vanish at absolute zero because the thermal-expansion coefficients become equal to zero (as required by the third law of thermodynamics). The secondary coefficient at 298 °K is in good agreement with the value of $21 \mu\text{C m}^{-2} \text{ }^\circ\text{K}^{-1}$ calculated by Jaffe.¹⁸ The relative signs of p_2^s and d_{22}^T were determined by a static piezoelectric test. The primary pyroelectric coefficients shown in Fig. 3 were then evaluated.

The validity of the assumptions in (i) and (ii) was tested by recalculation of the secondary pyroelectric coefficients assuming a quadratic temperature dependence of the elastic compliance and piezoelectric coefficients and a linear temperature dependence of the Grüneisen parameter. The magnitudes of the secondary pyroelectric coefficients were altered only slightly despite significant changes in the parameters of Eq. (2). Three reasons were found for this behavior: much term cancellation occurs in Eq. (2); the components d_{22}^T and C_{22}^T of the dominant term in expanded Eq. (2), $d_{22}^T C_{22}^T \alpha_2^s$, are so nearly temperature independent in the range 293–323 °K that the inclusion of reasonable quadratic temperature terms has little effect; and, the rapid decrease of the thermal-expansion coefficients with decreasing temperature weakens the effects of nonlinear temperature dependence in the other parameters.

Although the secondary coefficient of LSM is always positive, it is composed of the sum of 16 terms, some of which are negative; however, the positive term $d_{22}^T C_{22}^T \alpha_2^s$ so dominates the sum that no sign change results. Instead we find that the calculated primary pyroelectric coefficient is negative below 158 °K.

In the next section we interpret the behavior of the primary pyroelectric coefficient by means of some results of lattice dynamics.

LATTICE-DYNAMICS THEORY OF PRIMARY PYROELECTRIC COEFFICIENT

One of the first explanations of the pyroelectric effect based on nonclassical physics was presented by Boguslawski.¹⁹ His theory yielded an expression the temperature-dependent part of which was identical to the Einstein specific heat function²⁰:

$$E \left(\frac{\Theta_E}{T} \right) = 3R \left(\frac{\Theta_E}{T} \right)^2 \frac{e^{\Theta_E/T}}{(e^{\Theta_E/T} - 1)^2}, \quad (4)$$

where Θ_E is a characteristic Einstein temperature and R is the gas constant in $\text{cal g mole}^{-1} \text{ }^\circ\text{K}^{-1}$. Boguslawski found that this function fitted the higher-temperature pyroelectric data of Ackermann¹ rather well. He also used with some success a func-

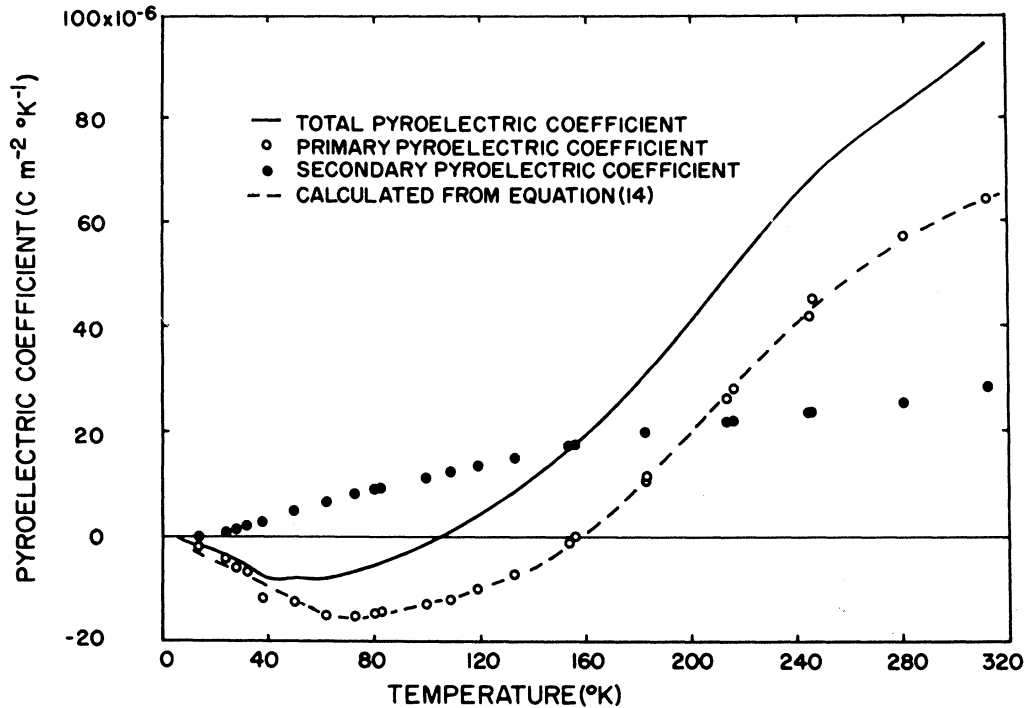


FIG. 3. The experimental total pyroelectric coefficient and primary and secondary coefficients determined at discrete points. The curve resulting from the least-squares fit of the primary pyroelectric points to Eq. (9) is superimposed on the points.

tion proportional to the Debye specific heat function²⁰:

$$D\left(\frac{\Theta_D}{T}\right) = 3RN\left(\frac{T}{\Theta_D}\right)^3 \int_0^{\Theta_D/T} \frac{x^4 e^x}{(e^x - 1)^2} dx, \quad (5)$$

where Θ_D is a characteristic Debye temperature and N denotes the number of oscillators per molecule (a single oscillator having three degrees of freedom). Boguslawski proposed that his functions were equally applicable to either total or primary pyroelectric data.

Max Born observed that pyroelectric data become linear with temperature at sufficiently low temperatures,²¹ requiring a functional form different from either an Einstein or a Debye function and necessitating a separation into the primary and secondary effects. The secondary pyroelectric coefficient has a T^3 dependence at low temperatures because of the thermal-expansion coefficients. By introducing a quantum-mechanical correction for deformations of the electron clouds surrounding the nuclei, he showed that the primary pyroelectric moment (polarization) of an oscillator was proportional, not to the energy of the oscillator, but to the mean square of the amplitude of the oscillation:

$$\langle A^2 \rangle \sim \frac{1}{\nu^2} \left(\frac{h\nu}{e^{h\nu/kT} - 1} \right), \quad (6)$$

where h , k , A , and ν represent Planck's constant, Boltzmann's constant, and the amplitude and frequency of oscillation, respectively. Upon summing these terms over the acoustical frequency spectrum, Born showed that the primary pyroelectric moment is proportional to the function

$$\left(\frac{T}{\Theta_D}\right)^2 \int_0^{\Theta_D/T} \frac{x dx}{e^x - 1}, \quad (7)$$

where Θ_D is the Debye characteristic temperature.

We first extend Born's result by differentiating Eq. (7) with respect to T [according to Eq. (1)] in order to calculate the primary pyroelectric coefficient:

$$\begin{aligned} \frac{p^\epsilon}{p_\infty^\epsilon} &= \frac{2T}{\Theta_D} \int_0^{\Theta_D/T} \frac{x dx}{e^x - 1} - \frac{\Theta_D/T}{e^{\Theta_D/T} - 1} \\ &\equiv B\left(\frac{\Theta_D}{T}\right). \end{aligned} \quad (8)$$

Several constants have been combined to form the new proportionality constant p_∞^ϵ . This function, here referred to as the Born function (B), is graphed with the Einstein and Debye functions in Fig. 4. Note that the Born function becomes linear in temperature as the temperature approaches zero.

In analogy to the temperature behavior of the heat

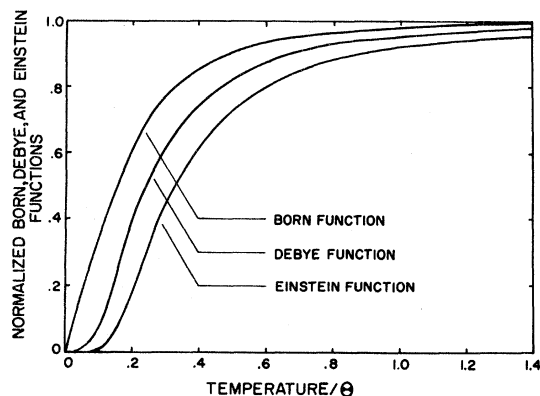


FIG. 4. Normalized Born, Debye, and Einstein functions. Note that the low-temperature behavior of the functions are linear, cubic, and proportional to $e^{-\Theta/T}$, respectively.

capacity, we propose that the Born function, Eq. (8), describes the primary pyroelectric coefficient at temperatures sufficiently low that only acoustical frequencies are excited. At higher temperatures optical-frequency vibrations contribute Einstein functions to the heat capacity.²⁰ Therefore, we propose that optical-frequency vibrations will contribute terms similar to Eq. (6) to the pyroelectric moment. However, the temperature-dependent part of the temperature derivative of Eq. (6) is also an Einstein function. Thus the primary pyroelectric coefficient is given by

$$p^e = p_\infty^e B\left(\frac{\Theta_D}{T}\right) + \sum_{i=1}^n C_i E\left(\frac{\Theta_{E,i}}{T}\right) \quad (9)$$

in complete analogy to the heat capacity described by

$$C_v = D\left(\frac{\Theta_D}{T}\right) + \sum_{i=1}^n E\left(\frac{\Theta_{E,i}}{T}\right). \quad (10)$$

Note that the coefficients in Eq. (9), because they are proportional to electric charges, can be either positive or negative, whereas the terms in Eq. (10) must always be positive.

The Debye and Einstein temperatures of LSM were found by fitting the heat-capacity data in Fig. 2 to Eq. (10). The experimental constant-pressure heat-capacity data were corrected to constant volume data by means of Eq. (3). The number of oscillators N was set equal to 3, considering three degrees of freedom for each of the two lithium ions and one for the hydrated sulfate ion. Five Einstein functions were required to describe the heat capacity at 300°K. A Fibonacci search technique was used to find first approximations to the six characteristic temperatures, and a pattern search method was used to converge to the final values.²² Only the value 265°K for the Debye temperature would give a good fit to the heat-capacity data, but a num-

ber of combinations of Einstein temperatures yielded satisfactory results. The best set of Einstein temperatures is given in Table I.

The Debye temperature was also calculated from elastic data using the equation²³

$$\Theta_D = \frac{h}{k} \left(\frac{9N}{4\pi VI} \right)^{1/3} \quad (11)$$

and

$$I = \int_0^{4\pi} \sum_{i=1}^3 \frac{1}{V_i^3} \frac{d\Omega}{4\pi}, \quad (12)$$

where V_i represents the velocities of propagation of the longitudinal and the two transverse acoustic waves, and Ω is an element of solid angle. Wave velocities were calculated from the Christoffel equations.²⁴ The integral in Eq. (12) was approximated by a summation over 2664 uniformly spaced directions. The resulting Debye temperature, 303°K, was in good agreement with the value found from heat-capacity data. Wave numbers corresponding to the five Einstein characteristic temperatures were calculated according to

$$\tilde{\nu} = (k/hc)\Theta_E, \quad (13)$$

where $\tilde{\nu}$ is the wave number in cm^{-1} and c is the velocity of light. Qualitative agreement was found between these wave numbers and the wave numbers of the ir absorption peaks²⁵ of LSM, as shown in Table I.

The primary pyroelectric coefficients calculated by means of Eq. (2) were fitted to Eq. (9) by least squares, yielding the following equation:

$$\begin{aligned} p_2^e = & -0.00001980 B(265/T) \\ & -0.00038739 E(589/T) \\ & +0.00980883 E(699/T) \\ & -0.01088382 E(717/T) \\ & +0.00174813 E(841/T) \\ & -0.00027735 E(1103/T). \end{aligned} \quad (14)$$

TABLE I. Comparison of wave numbers from Einstein temperatures and from ir spectra.

Θ_E (°K)	$\tilde{\nu}$ (calculated from Θ_E) (cm^{-1})	$\tilde{\nu}$ (ir) ^a (cm^{-1})	Intensity of ir band ^a
...	...	322	very weak
589	409	367	strong
699	486	437	weak, broad
717	498	480	weak, broad
841	585	577	very weak, broad
1103	767	646	strong

^aReference 25.

The average standard deviation of the experimental points from the theoretical line shown in Fig. 3 was $1.16 \mu\text{C m}^{-2} \text{K}^{-1}$, signifying very good agreement. We observed that small changes in the set of Einstein temperatures markedly increased this standard deviation, suggesting that the form of the equation does have theoretical significance. The occurrence of some self-cancelling terms in Eq. (14) is a result of the vanishing of p_2^2 at 158°K .

In summary, the same set of characteristic temperatures derived from heat-capacity data describes both the acoustic and optical spectra and the primary pyroelectric coefficient behavior reasonably well. Thus the Born theory of the pyroelectric coefficient is substantiated. Unfortunately LSM is a complex molecule which crystallizes in a very-low-symmetry solid, the structure of which is not readily amenable to theoretical calculations. It is suggested that similar experimental measurements and theoretical calculations be performed on a simpler molecule with higher crystallographic symmetry. A material having the hexagonal wurtzite structure, cadmium sulfide, for example, appears to be an attractive choice.

CONCLUSIONS

The following results and conclusions were found in this study:

1. The pyroelectric coefficient (at constant stress) of lithium sulfate monohydrate was determined over the temperature range $4.2\text{--}320^\circ\text{K}$. A sign change in the coefficient occurred at 106°K , as previously reported by Gladkii and Zheludev and in disagreement with the results of Ackermann.

¹W. Ackermann, *Ann. Physik* **46**, 197 (1915).

²V. V. Gladkii and I. S. Zheludev, *Kristallografiya* **10**, 10 (1965) [*Sov. Phys. Cryst.* **10**, 63 (1965)].

³R. Bechmann, *Proc. Phys. Soc. (London)* **65B**, 375 (1952).

⁴R. Bechmann, in *Landolt-Börnstein, Numerical Values and Functions*, 6th ed., edited by K. H. Hellwege (Springer, Berlin, 1966), Group III, Vol. 1, pp. 54, 60, 72, and 79.

⁵Standards on Piezoelectric Crystals, 1949, *Proc. IRE* **37**, 1378 (1949).

⁶W. P. Mason, *Crystal Physics of Interaction Processes* (Academic, New York, 1966), p. 131.

⁷C. S. Smith and H. H. Landon, *Phys. Rev.* **75**, 1625 (1949).

⁸S. B. Lang and F. Steckel, *Rev. Sci. Instr.* **36**, 929 (1965).

⁹S. B. Lang, S. A. Shaw, L. H. Rice, and K. D. Timmerhaus, *Rev. Sci. Instr.* **40**, 274 (1969).

¹⁰S. B. Lang, L. H. Rice, and S. A. Shaw, *J. Appl. Phys.* **40**, 4335 (1969).

¹¹S. B. Lang, M. D. Cohen, and F. Steckel, *J. Appl. Phys.* **36**, 3171 (1965).

¹²I. E. Paukov and M. N. Lavrent'eva, *Russ. J. Phys.*

The pyroelectric coefficient exhibited a broad extremum at 50°K and had a minimum value of $-0.1 \mu\text{C m}^{-2} \text{K}^{-1}$ at 4.2°K .

2. The total pyroelectric coefficient (under the constraint of constant stress) was resolved into the primary effect (pyroelectric effect at constant strain) and the secondary effect (piezoelectric effect caused by thermal strain). The total effect vanishes at 106°K because the primary and secondary effects cancel at that temperature. The secondary effect is positive at all temperatures and the primary effect is positive above 158°K .

3. The primary pyroelectric effect was interpreted theoretically by means of an extension of a lattice-dynamical theory proposed by Born. The primary pyroelectric moment (spontaneous polarization) consists of a sum of terms, each one proportional to the mean square amplitude of vibration of an intramolecular or intermolecular oscillator. The frequencies of the oscillators, expressed as one characteristic Debye temperature and five Einstein temperatures, were found from heat-capacity data. Good agreement was found between the primary pyroelectric coefficient data and a fitted curve, the terms of which were functions of the Debye and Einstein temperatures.

ACKNOWLEDGMENTS

The author acknowledges with thanks the financial support of the National Research Council of Canada. He also wishes to express his appreciation to the National Bureau of Standards, Institute of Basic Standards, Boulder, Colo., for the use of their laboratory facilities.

Chem. **43**, 775 (1969).

¹³J. F. Nye, *Physical Properties of Crystals* (Clarendon, Oxford, 1957).

¹⁴T. A. Perls, T. J. Diesel, and W. I. Dobrov, *J. Appl. Phys.* **29**, 1297 (1958).

¹⁵J. L. Wentz and L. Z. Kennedy, *J. Appl. Phys.* **35**, 1767 (1964).

¹⁶S. B. Lang, *Nature* **224**, 798 (1969).

¹⁷C. Kittel, *Introduction to Solid State Physics* 3rd ed. (Wiley, New York, 1966), pp. 165 and 183.

¹⁸H. Jaffe, *Phys. Rev.* **75**, 1625 (1949).

¹⁹S. Boguslawski, *Z. Physik* **14**, 569 (1914); **14**, 805 (1914).

²⁰J. C. Slater, *Introduction to Chemical Physics*, (McGraw-Hill, New York, 1939), pp. 199–255.

²¹M. Born, *Rev. Mod. Phys.* **17**, 245 (1945).

²²D. J. Wilde, *Optimum Seeking Methods*, (Prentice-Hall, Englewood Cliffs, N. J., 1964), pp. 24–30, 145–150.

²³H. B. Huntington, *Advan. Solid State Phys.* **7**, 213 (1958).

²⁴W. G. Cady, *Piezoelectricity* (Dover, New York, 1964), pp. 104–106.

²⁵F. A. Miller, G. L. Carlson, F. F. Bentley, and W. H. Jones, *Spectrochim. Acta* **16**, 135 (1960).